J. Fluid Mech. (1987), *vol.* 183, *pp.* 379–397
Printed in Great Britain

Vorticity and passive-scalar dynamics in two-dimensional turbulence

By ARMANDO BABIANO, CLAUDE BASDEVANT, BERNARD LEGRAS AND ROBERT SADOURNY

Laboratoire de Météorologie Dynamique du CNRS, Ecole Normale Supérieure, 75231 Paris Cedex 05, France

(Received 13 January 1986 and in revised form 27 March 1987)

The dynamics of vorticity in two-dimensional turbulence is studied by means of semi-direct numerical simulations, in parallel with passive-scalar dynamics. It is shown that a passive scalar forced and dissipated in the same conditions as vorticity, has a quite different behaviour. The passive scalar obeys the similarity theory *à la* Kolmogorov, while the enstrophy spectrum is much steeper, owing to a hierarchy of strong coherent vortices. The condensation of vorticity into such vortices depends critically both on the existence of an energy invariant (intimately related to the feedback of vorticity transport on velocity, absent in passive-scalar dynamics, and neglected in the Kolmogorov theory of the enstrophy inertial range); and on the localness of flow dynamics in physical space (again not considered by the Kolmogorov theory, and not accessible to closure model simulations). When space localness is artificially destroyed, the enstrophy spectrum again obeys a k^{-1} law like a passive scalar. In the wavenumber range accessible to our experiments, two-dimensional turbulence can be described as a hierarchy of strong coherent vortices superimposed on a weak vorticity continuum which behaves like a passive scalar.

1. Introduction

In the past twenty years, a number of theoretical, numerical and experimental studies have been devoted to the understanding of two-dimensional flow dynamics. Activity in this particular branch of fluid mechanics started when the self-similar Kolmogorov theory of turbulence was extended to two-dimensional flows by Kraichnan (1967), Leith (1968) and Batchelor (1969), who introduced the double-cascade concept, whereby enstrophy is carried from injection scales to small dissipation scales, while energy goes the other way and reaches ever larger scales in a supposedly infinite domain. A somewhat idealized picture of the two cascades as smooth, regular processes was later provided by closure-model calculations (Pouquet *et al.* 1975). But the whole theory remained somewhat academic in spite of its possible connections with atmospheric and oceanic large-scale flows (Wiin-Nielsen 1967; Desbois 1975; Morel & Larchevêque 1974) until truly two-dimensional flows were finally produced to a close approximation in laboratory experiments. Experimental evidence of the existence of reverse energy transfers was first obtained by Couder (1984) on thin liquid soap films, then by Sommeria (1985) in shallow mercury layer agitated by electrically driven vortices in a strong normal magnetic field. On the other hand, increasing computer power has led to accurate direct or semi-direct† numerical simulations of the enstrophy inertial range, which cannot at present be studied in the laboratory.

† Involving a parameterization of the transfers to sub-grid scales.

Long-term simulations of two-dimensional turbulent flows in forced or decaying conditions, performed by Fornberg (1977), Basdevant *et al.* (1981), McWilliams (1984) all led to the interesting result that the energy spectrum in the enstrophy inertial range or in decaying flows could significantly deviate from the k^{-3} law expected from the Kolmogorov theory. Indeed, slopes from k^{-4} to k^{-6} were obtained, depending on the nature of the forcing; and always associated with the emergence of strong solitary, long-lived, coherent vortices.

The similarity theory *à la* Kolmogorov (referred to as SK hereinafter) is too simple to account for the spectral variability and the spatial coherence obtained in numerical simulations: what we need is a more extensive understanding based on the multiplicity of actual flow behaviours. Indeed, the whole concept of two-dimensional turbulence reduces to vorticity advection and its feedback on velocity. Vorticity advection – the stretching of vorticity isolines by velocity shears – is relatively easy to handle with simple arguments; it is the feedback on velocity which is difficult to take into account. The SK theory succeeds in handling the dynamics of a passive scalar which exerts no feedback on the velocity distribution; but it apparently fails in describing vorticity dynamics, because it sees no difference with the passive-scalar dynamics. This difference between vorticity and passive-scalar dynamics is precisely the key to a deeper understanding of two-dimensional turbulence, and it is the purpose of the present work to evaluate it. We shall rely upon semi-direct simulations, an approach which differs from previous investigators (Holloway & Kristmannsson 1984; Lesieur & Herring 1985); these authors have mostly been using the statistical closure approach which does not take into account, for example, the capability of two-dimensional fluid dynamics to generate coherent vortices.

2. Basic equations

Incompressible fluid motion in two dimensions is governed by the vorticity equation

$$\frac{\partial \zeta}{\partial t} + \mathrm{J}(\psi, \zeta) = F_\zeta - D_\zeta. \tag{1}$$

Here ζ is the vorticity, ψ the stream function, J the Jacobian operator, F_ζ an external vorticity source and D_ζ the vorticity sink associated with dissipation. Equation (1) shows that vorticity is simply advected by the flow in the absence of sources and sinks. In that case ($F_\zeta - D_\zeta = 0$), energy

$$E = \int\int_\Omega -\tfrac{1}{2}\psi\zeta \,\mathrm{d}x\,\mathrm{d}y, \tag{2}$$

and enstrophy

$$Z = \int\int_\Omega \tfrac{1}{2}\zeta^2 \,\mathrm{d}x\,\mathrm{d}y \tag{3}$$

are quadratic invariants of the motion; in (2) and (3) Ω is the flow domain.

The evolution of a passive scalar, or pollutant density ξ, is governed by an equation formally identical with (1):

$$\frac{\partial \xi}{\partial t} + \mathrm{J}(\psi, \xi) = F_\xi - D_\xi, \tag{4}$$

with corresponding pollutant sources and sinks; in their absence ($F_\xi - D_\xi = 0$), (4) also has a quadratic invariant

$$X = \int\int \tfrac{1}{2}\xi^2 \,\mathrm{d}x\,\mathrm{d}y, \tag{5}$$

which means that, like enstrophy, the total variance of the pollutant density is conserved.

The important difference between (1) and (4) is that ζ and ψ in (1) are related by $\zeta = \nabla^2\psi$, while ξ and ψ in (4) are not related to each other. For this reason (4) has no invariant analogous to (2); or in other words, the correlation

$$F = \int\int_{\Omega} -\tfrac{1}{2}\psi\xi \,\mathrm{d}x\,\mathrm{d}y \tag{6}$$

is not an invariant of the motion, even in the absence of sources and sinks. We shall see later that this rather obvious difference is in fact extremely important, as it induces fundamentally different dynamical properties for the two apparently identical equations (1) and (4): the 'active' scalar ζ and the 'passive' scalar ξ will be seen to behave in quite different ways.

Another important property of (1) and (4), now taken together, is the invariance of the correlation

$$R = \int\int_{\Omega} \tfrac{1}{2}\zeta\xi \,\mathrm{d}x\,\mathrm{d}y \tag{7}$$

in the absence of sources and sinks. More generally if

(i) the active and passive scalars ζ and ξ are initially decorrelated ($R = 0$ at $t = 0$);

(ii) there is no correlation source;

(iii) dissipation takes the general form

$$D_\eta = \mathrm{D}(\psi)\,\eta, \tag{8}$$

where $\mathrm{D}(\psi)$ is a linear, symmetric (positive definite) operator; then R remains zero at all times: ζ and ξ are free to evolve in quite different ways. Note that condition (iii) is generally verified by artificial viscosity schemes used in numerical models: for instance, the linear viscosity defined by an iterated Laplacian

$$D_\eta = \tau^{-1}(-\lambda^2\nabla^2)^n\,\eta \tag{9}$$

(Basdevant *et al.* 1981), or a nonlinear viscosity like the 'anticipated vorticity' scheme (Sadourny & Basdevant 1981, 1985):

$$D_\eta = \tau\mathrm{J}(\psi, (-\lambda^2\nabla^2)^n\,\mathrm{J}(\psi,\eta)); \tag{10}$$

here τ and λ are the characteristic time- and lengthscales associated with the numerical cutoff.

3. Similarity theory, stability theorems and closure models

The SK theory is not quantitative enough to distinguish between vorticity and a passive scalar. Taking for example the case of a stationary two-dimensional turbulence forced at wavenumber k_I with injection rates e (for energy) and $z = k_\mathrm{I}^2 e$ (for enstrophy), we obtain the SK estimate of the one-dimensional enstrophy spectrum $Z(k)$ in the enstrophy inertial range by equating the constant enstrophy cascade rate z to the enstrophy available at wavenumber k, divided by the characteristic time of nonlinear transfers $\tau(k)$:

$$z = \frac{kZ(k)}{\tau(k)}; \tag{11}$$

$\tau(k)$ is estimated from a root-mean-square measure of velocity gradients at scales larger than k^{-1}:

$$\tau(k) = \left(\int_0^k Z(p)\, \mathrm{d}p \right)^{-\frac{1}{2}}. \tag{12}$$

Elimination of $\tau(k)$ between (11) and (12) yields the familiar enstrophy spectrum (Kraichnan 1971)

$$Z(k) = Cz^{\frac{2}{3}}k^{-1}(\ln k)^{-\frac{1}{3}}. \tag{13}$$

It can be shown (Monin & Yaglom 1965, §22; and Frisch 1987) that relation (11) relies on the assumption that the scale invariance of the Euler equation is recovered within the inertial range. Indeed, scale invariance appears violated in dimension two by relation (12), which introduces the logarithmic correction to the power law observed in (13). More importantly, the derivation of (13) is independent of the existence of an energy invariant, or in other words, of the physical relationship between ψ and ζ which embodies the feedback of vorticity dynamics on velocity. Precisely for this reason, the same argument, applied to a passive scalar ξ injected at the same wavenumber k_{I}, yields the same spectral distribution (Lesieur & Herring 1985). Denoting by $X(k)$ the one-dimensional power spectrum of ξ and by x its cascade rate, we write instead of (11)

$$x = \frac{kX(k)}{\tau(k)}, \tag{14}$$

and, by eliminating $\tau(k)$ and $Z(k)$ between (12), (13) and (14),

$$X(k) = C'z^{-\frac{1}{3}}xk^{-1}(\ln k)^{-\frac{1}{3}}. \tag{15}$$

This complete analogy of behaviour between vorticity and the passive scalar is likely to be a gross oversimplification owing to the limitations of the SK theory, as the feedback of vorticity transport on velocity clearly brings very strong constraints on vorticity dynamics. We know from simple examples dealing with parallel flows that vorticity gradients may have a stabilizing effect on smaller-scale vorticity structures. This is readily seen from the linear stability theory (e.g. Lin 1967) which yields, as a necessary condition for instability, the vanishing of the vorticity gradient across the mean flow, a result recently confirmed in the fully nonlinear case, by a Liapunov stability theorem derived by McIntyre & Shepherd (1987) – see also Shepherd (1987). It is quite clear from both demonstrations that such stability results are crucially dependent on the ψ–ζ relationship; they are specific of vorticity dynamics and do not hold for the scalar. For more general (not necessarily parallel) quasi-stationary flows, one stabilizing mechanism appears to be the tendency of a vorticity gradient to induce a propagation of smaller-scale perturbations of the vorticity field towards its left. This propagation is ordinarily mixed with straining, except in the limiting case of the pure beta-effect on the beta-plane. Several authors (Rhines 1975; Holloway & Hendershott 1977; Legras 1980) have shown that the beta-effect indeed inhibits energy or enstrophy transfers, one of the consequences being a steepening of the spectral slope in the enstrophy inertial range. It is therefore quite possible that, even in the absence of an external beta-effect, the presence of quasi-stationary internal vorticity gradients, by mixing straining with propagation, induce comparable inhibitions of enstrophy transfers across the inertial range, steepening the spectral slope beyond the SK expectation.

Closure models are much more quantitative than the SK theory: they involve triad interaction coefficients which differ in the vorticity and passive-scalar cases, because

of the symmetry properties associated with the ψ–ζ relationship. We may thus expect them to represent, at least up to some point, these statistical stabilizing effects of vorticity gradients. This has indeed been verified by Holloway & Kristmannsson (1984); however, these authors, like Lesieur & Herring (1985) have found identical asymptotic behaviour for enstrophy and passive-scalar variance, except perhaps for differences in the values of the multiplicative constants. This can be readily understood if we note that, in the enstrophy inertial range of a closure model, the enstrophy transfer through wavenumber k is mainly due to a set I of non-local interactions (k', p, q) with $q \ll k' < k < p$; while the energy conservation is recovered by an inverse flux due to a separate set II of interactions with $k' \ll k < p \approx q$: on this point, see for instance Basdevant, Lesieur & Sadourny (1978). Interactions of type I transfer enstrophy and passive-scalar variance in the same way; on the other hand, the enstrophy transfer associated with interactions of type II (i.e. with the presence of an energy invariant, or with the ψ–ζ relationship, or in other words, with the feedback of vorticity transport on velocity) is negligible. Thus, asymptotically, the closure models will not distinguish between passive scalars and vorticity.

4. A numerical experiment

A forced stationary, turbulent, two-dimensional incompressible flow regime is first simulated using a 128×128 point spectral model on the $2\pi L$-periodic plane (Basdevant *et al.* 1981). Forcing is imposed by assigning a constant value to the amplitude of a given Fourier mode, here $\sin 4y_1/L$. Dissipation includes a large-scale 'friction' in addition to the iterated Laplacian (9) with $n = 8$:

$$D_\zeta = \left(\frac{1}{\theta}(-\lambda^2 \nabla^2)^8 - \frac{1}{\theta} L^{-2} \nabla^{-2}\right)\zeta. \tag{16}$$

The first term in the bracket is designed mainly to dissipate enstrophy at the largest resolved wavenumbers ($k < \lambda^{-1}$) with a timescale equal to the eddy-turnover time at the cutoff scale λ: $\theta = \tau(\lambda^{-1})$. The second term mainly dissipates energy at the largest scales ($k > L^{-1}$) with a time scale θ'. This model was integrated from initial conditions characterized by an exponentially decaying spectrum and random phases. The numerical integration was pursued long enough to reach a stationary regime for the enstrophy spectrum. The instantaneous enstrophy spectrum at a time $t = t_0$ of this stationary final regime is shown in figure 1; it practically does not vary thereafter. We note that in contrast to the prediction (13), this enstrophy spectrum can be much steeper than k^{-1} (here for $20 < k < 50$), a behaviour already observed in numerical experiments by several authors, including Fornberg (1977), Basdevant *et al.* (1981) and McWilliams (1984). Also, as reported by all these authors, the vorticity chart at $t = t_0$ (figure 2*a*) is remarkable by the presence of a number of strong, isolated, quasi-circular vortices, which have very long lifetimes compared to the more turbulent-like surrounding structures.

These features are shared by a large number of numerical simulations performed with a wide range of forcing mechanisms, deterministic or random (Basdevant *et al.* 1981), or a large class of initial conditions in the case of decay experiments (McWilliams 1984). Basdevant *et al.* (1981) have shown that they persist in the presence of the β-effect, although a strong tendency towards zonal anisotropy is also observed in this case. It has been suggested by Herring & McWilliams (1985) that the wavenumber span $0 < k < 64$ was too small to adequately test an inertial range.

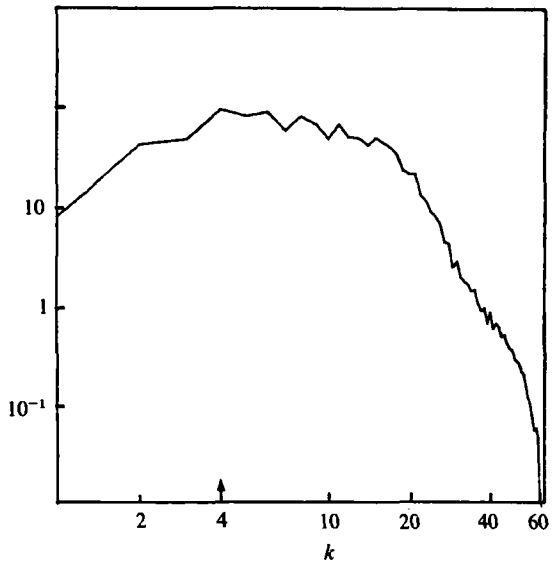

FIGURE 1. Enstrophy and passive-scalar variance spectra at $t = t_0$, when $Z(k, t_0) = X(k, t_0)$. The arrow indicates the injection wavenumber.

They show that a closure model, known to develop a k^{-1} range at high resolution, exhibits a k^{-2} slope with our resolution. This behaviour might be characteristic of the closure approach as the authors show also that direct numerical simulations yields the same k^{-2} spectrum in resolutions 128×128 and 256×256. Basdevant *et al.* (1981) computed the enstrophy fluxes and found them to be constant over the whole range of the observed power law; this is probably the best proof of the existence of an enstrophy inertial range. We must agree however that the present resolution, although perhaps sufficient to study the large-scale dynamics, does not allow a direct test of asymptotic laws at small scales and that the observed slopes may differ in a more extended enstrophy inertial range. This is why we give here (equation (17)) a technique to test the Kolmogorov theory precisely, even at a moderate resolution like ours.

A more serious question arises from the observation of k^{-1} enstrophy spectra reported recently in high-resolution decay experiments by Brachet, Meneguzzi & Sulem (1986) and Kida (1985). In these simulations, there is no generation of coherent vortices, but instead, an iterative piling up of vortex sheets which prevents the generation of steeper spectra. We must observe that, starting from flows initially confined to the largest scales, these experiments might have been integrated for an insufficiently long time to develop vortex structures. Indeed, some very recent computations (Santangelo, Paternalo & Benzi 1987; R. Benzi, private communication) suggest the existence of a metastable k^{-1} regime in which a decay flow may enter provided its initial spectrum is sufficiently steep, and whose duration increases with the Reynolds number.

At time $t = t_0$, a passive scalar ξ was injected into the flow. The initial condition for ξ was defined by taking the vorticity field at $t = t_0$, and keeping constant the amplitudes of all Fourier modes while resetting phases at random. The initial spectra $X(k, t_0)$, $Z(k, t_0)$ are therefore identical (figure 1), but the correlation $R(k, t_0)$ is close

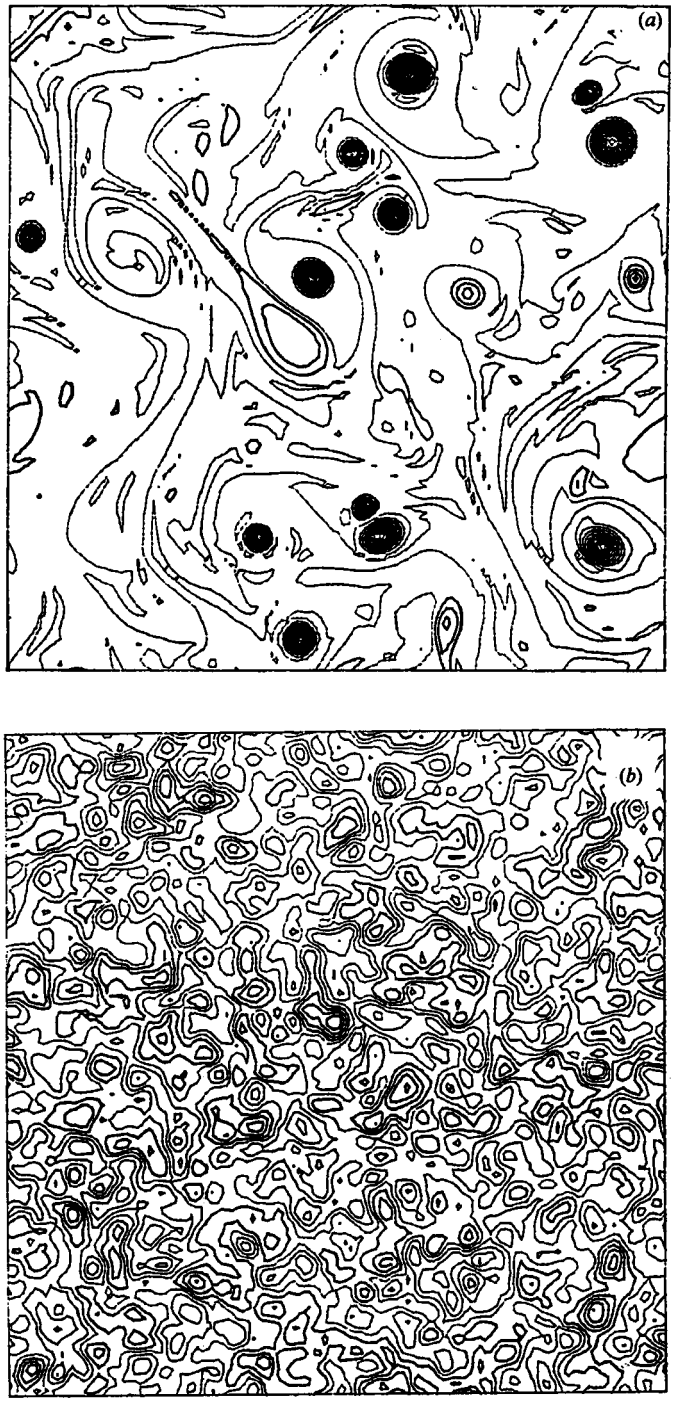

FIGURE 2. (*a*) Vorticity and (*b*) passive-scalar fields at $t = t_0$.

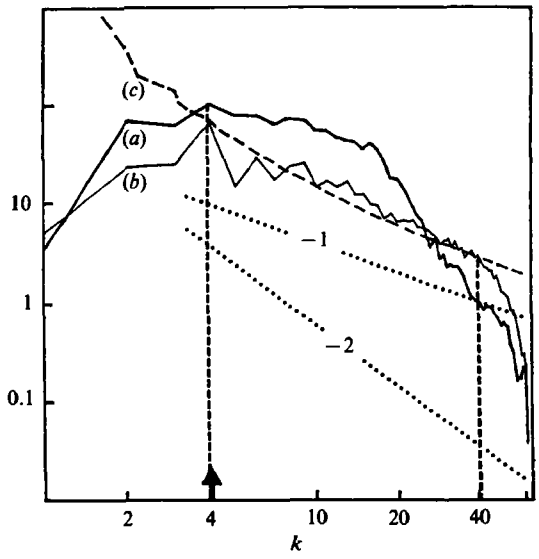

FIGURE 3. (a) Enstrophy and (b) passive-scalar variance spectra at $t = t_1$; the third spectrum (c) is the Kolmogorov estimate $X'(k)$. The arrow indicates the injection wavenumber.

to zero. Figure 2(b) shows the passive-scalar field at $t = t_0$: all the organized structures visible in figure 2(a), in particular the circular vortices, have been destroyed by the random phase shifts. From t_0 onward, ξ was forced like ζ, by holding the amplitude of its Fourier mode $\cos 4y_1/L$ constant; thus X and Z are injected at the same scale, but the correlation source is zero. Finally, ξ was dissipated exactly like vorticity, using the same operator (16) with the same timescales. We have seen in §2 that for such initial, forcing and dissipation conditions, R will remain close to zero at all times. Therefore, in the course of our simulation, ξ and ζ remain approximately decorrelated although their evolution is governed by strictly identical equations. The only difference between the two quantities is that ξ is passive with respect to the flow (in other words, independent of ψ), while ζ is not.

The ζ- and ξ-equations were thus integrated from $t = t_0$ onward, until a stationary regime was found for the passive-scalar spectrum. Figure 3 shows the two spectra $Z(k, t_1)$, $X(k, t_1)$ at a time $t = t_1$ within this stationary regime. The two spectra, which were identical at $t = t_0$ (figure 1), have now departed significantly from each other. As expected, $Z(k)$ has not varied much from t_0 to t_1; but $X(k)$ has lost most of its initial steepness, being now close to the k^{-1} law of the SK theory. Note however that (15) was established using (13), which is not verified by our calculations: therefore, the whole argument is at fault, in the form used in §3, and we cannot test directly the observed spectrum for the passive scalar against (15).

We may however reformulate the SK theory in a weaker form in order to show its validity for the passive-scalar dynamics. We do this in the following way: first we compute a direct estimate of the characteristic transfer time $\tau'(k)$ in our model flow by applying (12) to the simulated enstrophy spectrum $Z(k, t_1)$; then we compute an estimate of the passive-scalar spectrum $X'(k)$ by using the basic relation (14):

$$X'(k) = xk^{-1}\tau'(k). \tag{17}$$

$X'(k)$ is shown in figure 3, together with $Z(k, t_1)$. It behaves asymptotically as k^{-1}, due to the fast decrease of $Z(k, t_1)$ which ensures rapid convergence of the integral

in (12). The fact that $X'(k)$ is asymptotically independent of the slope of $Z(k)$ as soon as the latter decreases fast enough with k must be put in relation to the saturation effect of structure-function slope under the same condition (Babiano, Basdevant & Sadourny 1985). Moreover, it fits the simulated passive-scalar spectrum $X(k, t_1)$ rather well in the wavenumber band (k_1, k_D) when multiplied by an appropriate constant. The present technique allows a much better verification of the SK theory than the usual simpler technique of direct exponent fitting, which would have led here to an apparently steeper law. It tells us that the computed variance spectrum of the passive scalar is indeed consistent with the form expected from (15).

5. The mechanisms of coherent vortex formation

The comparison of vorticity and pollutant charts at $t = t_1$ (figure 4) sheds some light on this disparity of spectra. In terms of shape of the isolines the two fields are quite similar, which must be expected as they are both strained by the same velocity field. Note that in spite of the similarity of shapes, the correlation R remains close to zero, because the sign of the passive scalar is not correlated to the sign of vorticity. The main difference between the two fields lies in the distribution of the intensity of structures. As already mentioned, the vorticity field is dominated by strong coherent quasi-circular vortices whose high level of excitation contrasts with the relativity weak, elongated, 'turbulent' – like structures filling the remaining space. Nothing similar is observed in the scalar field, which does not accumulate within the vortices but is essentially carried, strained and mixed by the vortices in the background region. A consequence of this, clearly visible in figures 10 and 11 of Holloway & Kristmannsson (1984), is that a spot of scalar which does not initially intersect any vortex, in their words, 'homogenizes rather ineffectively despite the fact that tracer has been dispersed over scales larger than characteristic eddy fields'.

The generation of coherent vortices seems to be a generic property of two-dimensional turbulence, associated with steep spectra. Coherent vortices can emerge from random forcing or random initial conditions, as observed by Basdevant *et al.* (1981) in the stationary forced case, or McWilliams (1984) for decaying flow. They are remarkably stable, being able to maintain themselves for as long as several hundreds of their own eddy-turnover times. Their quasi-circular shape makes them close to local solutions of the Euler equation in which the nonlinear term is strongly inhibited. However, they occasionally undergo non-axisymmetric oscillations (McWilliams 1984) without loss of stability. The presence of coherent vortices always leads to spectra steeper than expected from the classical prediction. Studying their emergence in two-dimensional decaying turbulence, McWilliams (1984) traces them back to initial vorticity maxima, describing them as structures robust enough to be unaffected by the enstrophy cascade. In forced two-dimensional turbulence, coherent vortices seem to be generated in the enstrophy-cascading inertial range: all vortices observed in figure 2(*a*), for example, have scales smaller than the injection scale. Vortices are observed at various scales, but we have to wait for really high-resolution experiments to decide whether or not there can be a full hierarchy of vortices at all scales, throughout the whole enstrophy inertial range. What happens in the energy inertial range – a question of interest for atmospheric and oceanic dynamics – remains a widely open question; very few studies (Frisch & Sulem 1984) have tackled the problem of simulating properly the reverse energy cascade.

Stability is of course the key question of coherent vortex dynamics. For a passive scalar superimposed on a circular vortex, any non-axisymmetric perturbation

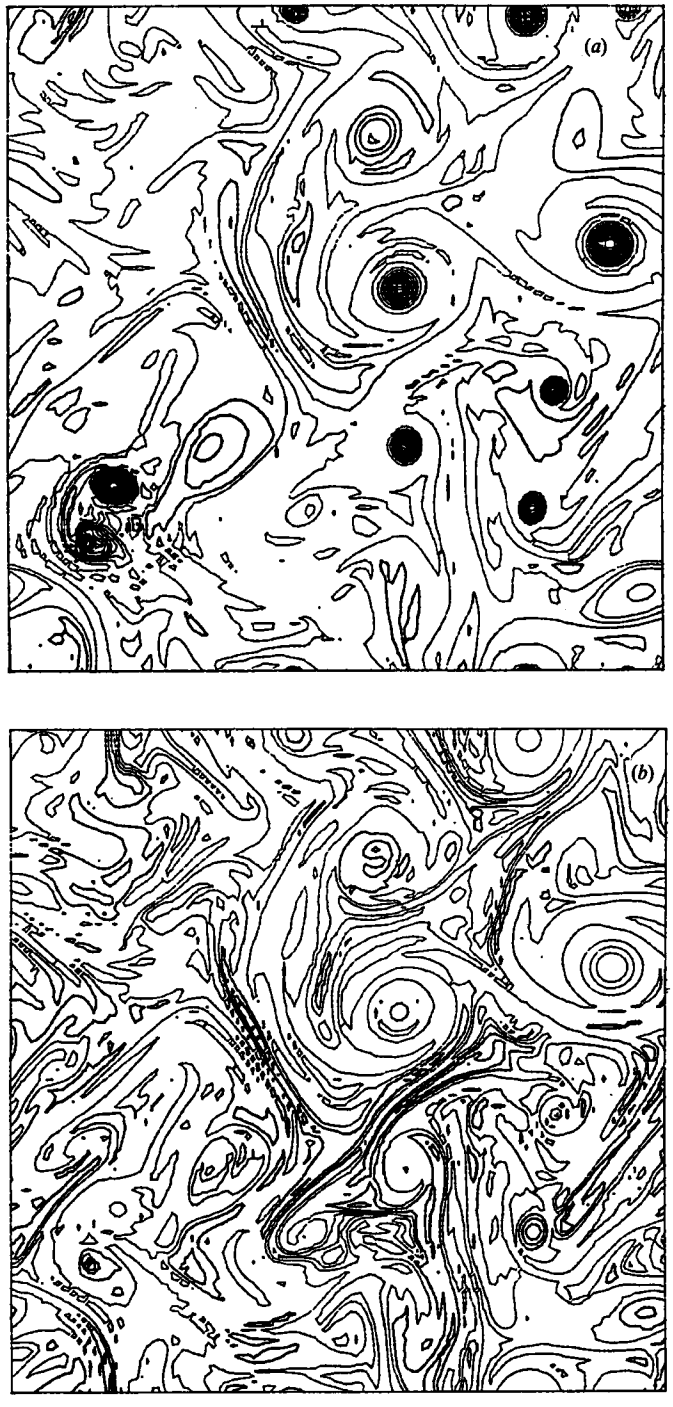

FIGURE 4. (*a*) Vorticity and (*b*) passive-scalar fields at $t = t_1$.

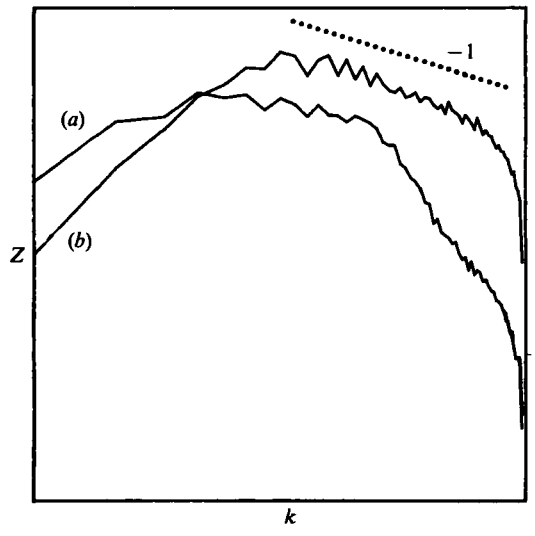

FIGURE 5. Enstrophy spectra from the 'random phase' model experiment: (*a*) at $t = t_0$; (*b*) at $t = t_1$. The -1 slope is indicated.

induces a rapid diffusion by shear mixing (Rhines & Young 1983) if the vortex is not a solid rotation; this eventually leads to complete homogeneization of the passive scalar inside the vortex.† A similar behaviour has been predicted by Rhines & Young (1982) for vorticity itself, i.e. that the eddy flux of vorticity would tend to dissipate the mean gradient. Numerical simulations lead us to the opposite conclusion, that non-uniform vorticity concentrations are generated and maintained through up-gradient eddy vorticity fluxes. Indeed, vorticity differs from a passive pollutant in the fact that any perturbation of vorticity means an advective perturbation which may eventually restore equilibrium (see §3). In this process the local correlation between stream function and vorticity (which on the global scale corresponds to the energy invariant, non-existent in passive-scalar dynamics) must play an important role.

Leith (1985) has provided an enlightening description, or even explanation, of coherent vortices in terms of his 'minimum enstrophy vortex' model, whose structure minimizes the enstrophy for given energy and angular momentum. Coherent vortices appear to be generated by systematic interaction‡ of eddies of the same sign (while eddies of opposite sign just move around each other without merging). Vortex build-up through single-sign eddy interaction is a slow local reverse energy cascade process: the two necessary ingredients for coherent vortex formation are energy conservation (or more precisely: feedback of vorticity advection on velocity), and the fact that straining processes are local in physical space (see again §3). These two properties are obviously overlooked in the SK theory of the enstrophy inertial range,

† However, in a decay flow with the same diffusion applied to the passive scalar and the vorticity, a passive scalar with an initial distribution proportional to the vorticity conserves this property throughout the evolution.

‡ The difference between interaction and simple aggregation must be clearly stated. Patches of quasi-uniform vorticity concentration occasionally occur in numerical simulations, but they remain clearly distinguishable from coherent vortices; in particular, their lifetime is relatively short, owing to weak stability.

which explains its inadequacy in the fact of numerical simulations. We must look at coherent vortices as local terminations of reverse energy cascade processes within the enstrophy inertial range, reaching an orderly robust shape, strong enough to become unperturbed by the relatively weak surroundings upon which it has already fed, and thus being unable to reach the scales of the energy inertial range (Sadourny 1985).

There is no such thing as an energy invariant for the passive scalar, hence no reverse energy cascade. This is why we do not obtain, in the pollutant field, anything resembling the coherent vortices. The other way to break the coherent-vortex generation is to disrupt the locality of straining processes in the physical space, which again destroys the local stabilizing effect of vorticity gradients. This can be illustrated by the following experiment: we take the same model of the two-dimensional Navier–Stokes equation as used for the control simulation, with the same initial conditions, forcing and dissipation, but at every time-step, we destroy the spatial coherence by resetting the phases of all Fourier modes at random. Since we keep constant the amplitudes of all modes, the perturbed model remains energy and enstrophy conserving but its ability to generate coherent structures is of course totally disrupted, exactly like a statistical closure model. The spectrum produced in the stationary regime of this 'random-phase' model is shown in figure 5: it indeed follows the SK law in k^{-1}. Note that the random-phase model has exactly the same quasi-normal closure as the original equations: EDQNM theory would therefore be unable to explain the very steep spectrum obtained in our numerical experiments. The steep spectrum here is the spectral signature of coherent vortices, whose description is beyond the reach of closure models.

6. Exploring the turbulent medium

The coherent vortex emerging from disorganized turbulent surroundings is a relatively vague notion which needs clarification by a quantitative approach. The two characteristic properties which at first sight identify the coherent vortex are its relatively high level of excitation and its relatively round shape. There is however no obvious threshold value that would unambiguously characterize it in terms of excitation level; and on the other hand, its shape constantly undergoes slight vacillations as the vortex interacts weakly with the turbulent medium. One possible way to separate the coherent vortex from its surroundings is to use an *a priori* model such as Leith's (1985) minimum enstrophy vortex model, and fit it to the vorticity field in some root-mean square sense. Here we shall follow a cruder but simpler approach, which will nevertheless bring out some interesting conclusions concerning the underlying structure of the turbulent field.

Taking advantage of the facts that coherent vortices occupy a small portion of space and have much stronger amplitudes than the remaining field, we may try to get rid of them by just 'clipping' the vorticity field. We call the following operation performed on a scalar field $\eta(x,y)$ 'clipping', and it is meant to suppress all values in excess of a given parameter $a > 0$:

$$\eta_a(x,y) = \begin{cases} a & \text{if } \eta(x,y) > a, \\ \eta(x,y) & \text{if } -a < \eta(x,y) < a, \\ -a & \text{if } \eta(x,y) < -a. \end{cases}$$

At first sight, applying the clipping operation to the vorticity field is not a clean way of suppressing vortices, but we shall nevertheless try it. Let us first clip the

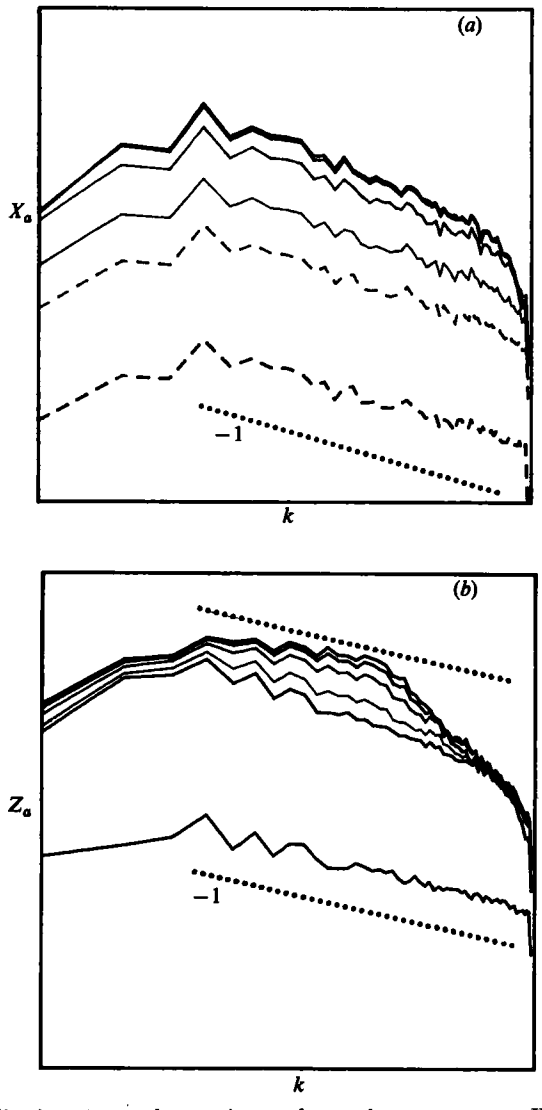

FIGURE 6. Effect of clipping: (*a*) on the passive-scalar variance spectrum $X_a(k)$. From top to bottom: $a = 1, \frac{1}{2}, \frac{1}{4}, \frac{1}{10}, \frac{1}{20}, \frac{1}{100}$ the maximum value of $|\xi|$. (*b*) On the enstrophy spectrum $Z_a(k)$. From top to bottom: $a = 1, \frac{1}{2}, \frac{1}{3}, \frac{1}{6}, \frac{1}{12}, \frac{1}{600}$ the maximum value of $|\zeta|$. The -1 slope is indicated.

passive-scalar field; the result in terms of power spectra $X_a(k)$ for various values of a is shown in figure 6(*a*). The striking fact is the robustness of the k^{-1} law to the clipping operation. Even more importantly, we see that strong clipping preserves local fluctuations around the mean slope, but destroys the high-wavenumber bias due to the artificial dissipation range, and the low-wavenumber bias due to the fact that the k^{-1} law is only asymptotic (remember figure 3 and the $X'(k)$-behaviour). It thus seems that the very crude technique of clipping indeed preserves the memory of the underlying k^{-1} law, even for very small a when the only memory of the field is its sign or in other words the shape of the zero isoline.†

† Notice that the singularities in the derivatives of the vorticity field induced by the clipping produce a k^{-4} enstrophy spectrum which can hardly mask a k^{-1} spectrum.

Clipping now the vorticity field (figure 6*b*), we observe a very different spectral behaviour, with strong sensitivity of the spectral shape for relatively large values of a. As a increases, the steep spectral slope rapidly levels off, and the clipped enstrophy spectrum converges to a clean k^{-1} law just like the passive scalar. This is consistent with our previous remarks that the passive scalar and vorticity have almost coincident isolines, and that the shape of the zero isoline is a remarkably good indicator of a k^{-1} spectral slope. Obviously the clipping process first destroys the strong coherent vortices, which explains the initial sensitivity of the spectrum to decreasing a; what remains afterwards (the shape of isolines) is the indicator of the surrounding medium. This shows that the medium that surrounds the coherent vortices in the vorticity field is indeed a field of passive-scalar type with its underlying k^{-1} law: the dynamical interpretation of this behaviour is straightforward.

7. The enstrophy cascade revisited

We now see the turbulent medium inbetween vortices as a passive field mainly strained by a set of isolated vortices which contribute most of the energy in the spectrum and therefore, determine the straining timescale. In figure 7, we show the spectral fluxes of enstrophy and passive-scalar variance in two experiments, the experiment described above and another one where the forcing was set at wavenumber 10 instead of wavenumber 4; all fluxes shown on figure 7 are instantaneous fluxes taken at the same time $t = t_1$. We see that the same straining is more efficient at transferring passive-scalar variance than at transferring enstrophy. This is consistent with the fact that coherent vortices are structures that tend to protect themselves from enstrophy dissipation. The higher efficiency of passive-scalar transfers was noticed by Holloway & Kristmannsson (1985), who gave the case of a narrowband spectrum as a typical example. This perhaps unrealistic situation is easily superseded by the existence of local relations between the vorticity and the stream function in the domain spanned by the vortices. We also note that the fluxes of pollutant variances are smoother than the enstrophy fluxes: this is again understandable, because in the flow dynamics, the relatively smooth enstrophy cascade which takes place in the turbulent medium is not efficient enough and must be supplemented by relatively intermittent inelastic interactions taking place among a limited number of isolated vortices.

The most dramatic vortex interaction is the collision of two vortices of the same sign, which produces a coalescence into a single new vortex. Conversely the interaction between two vortices of opposite sign is non-destructive and generally temporary. The addition of the velocity field of the two vortices generates a strong velocity along the axis; the couple then travels under its own velocity field, much faster than the characteristic velocity of the turbulent medium: the two vortices are then unable to interact and will eventually separate without major deformation when encountering other vortices (Basdevant, Couder & Sadourny 1985). The pairing mechanism, here observed in homogeneous conditions, was observed in shear flows by Winant & Browand (1974) and numerically simulated by several authors (see for instance Corcos 1983; Staquet & Lesieur 1987). Vortices of the same sign, on the contrary, interact as shown in figure 8 (see also McWilliams 1984): they turn around each other, getting closer and closer until they finally aggregate, expelling enstrophy along vorticity spirals. The whole process is a clear illustration of the reverse energy cascade, locally associated with the cascade of enstrophy: the resulting vortex of figure 8(*f*) has a larger scale than the two incident vortices of figure 8(*a*).

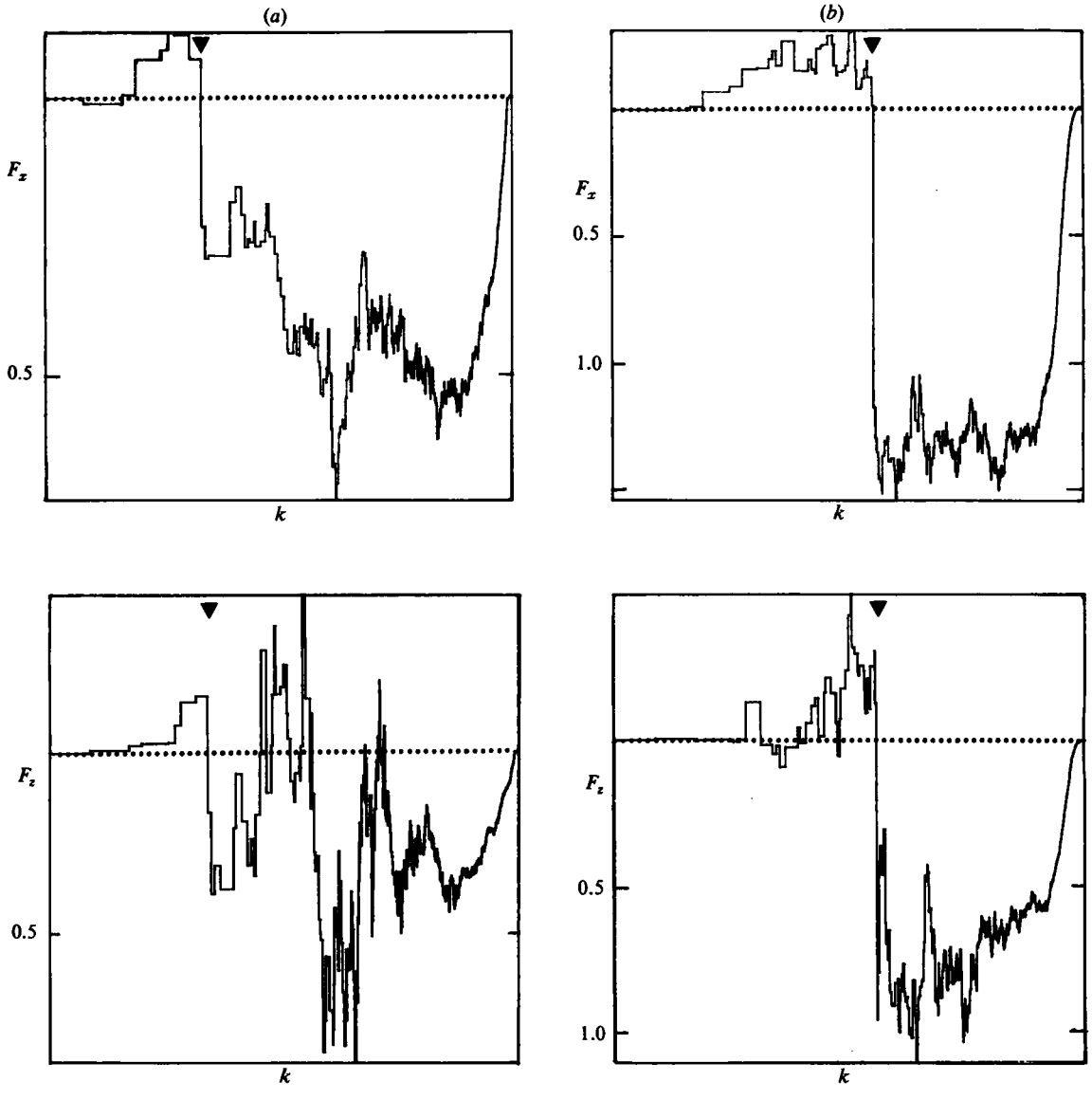

FIGURE 7. Enstrophy (F_z) and passive-scalar (F_x) fluxes in spectral space at $t = t_1$, for the two experiments (*a* and *b*). All fluxes are counted positively towards large scales.

8. Conclusion

The simple similarity theory *à la* Kolmogorov sees no difference between vorticity and passive-scalar dynamics. What we have tried to show here is that this difference is indeed the key point for deriving a more realistic theory. We have shown for example, that the unexpectedly steep spectra obtained in numerical simulations of the enstrophy inertial range, are not observed in the case of a passive scalar, forced and dissipated in strictly similar ways. A major difference between passive scalars and vorticity consists in the capacity of the latter to organize itself into sporadic, strong, coherent vortices. These vortices are relatively stable structures, generated

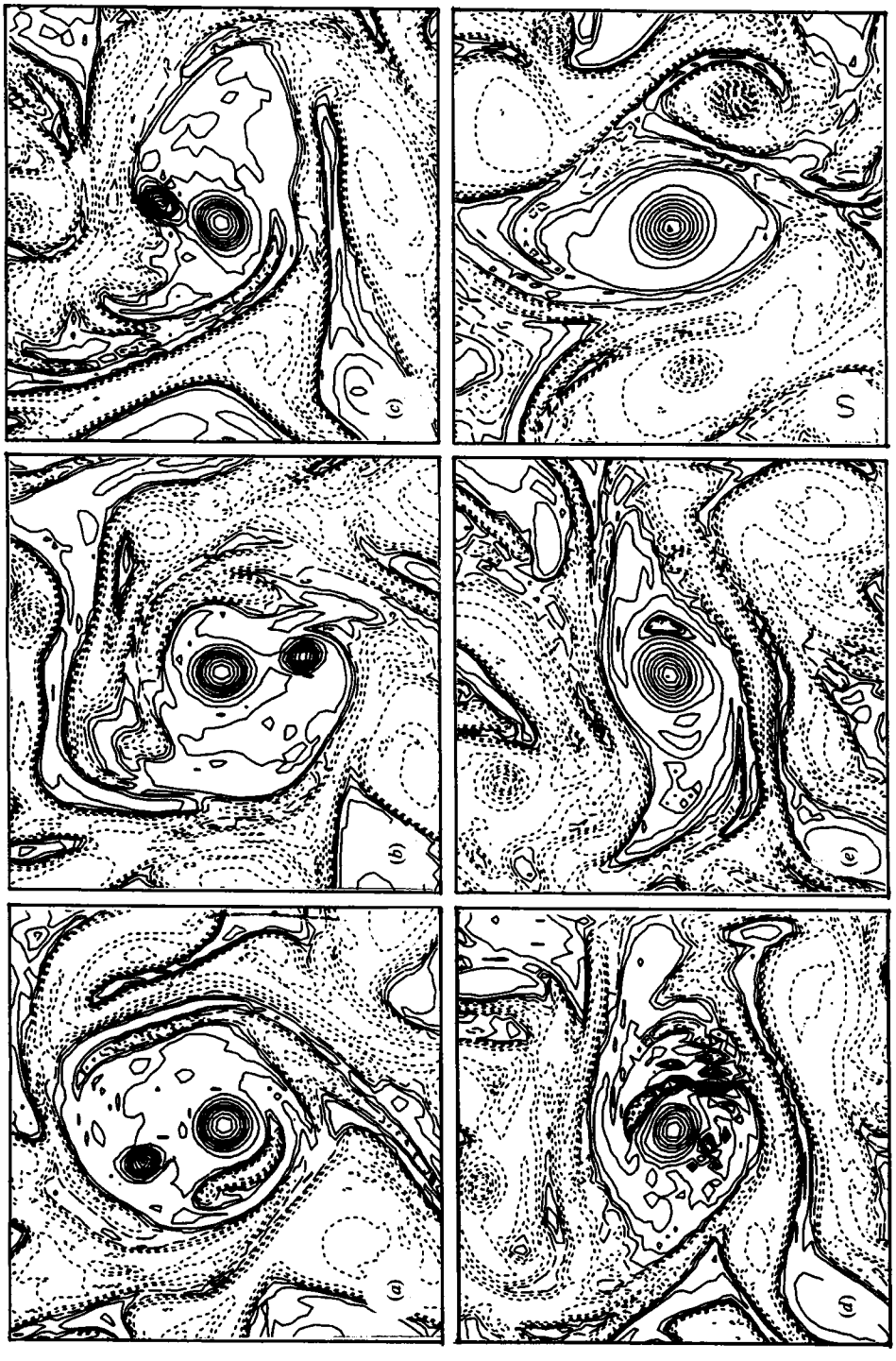

FIGURE 8. Time sequence showing the interaction of two positive vortices, and their coalescence into a more energetic, larger-scale vortex. The isolines are evenly spaced on a logarithmic scale, which allows a thorough description of the surrounding medium.

and maintained against enstrophy cascade and dissipation by up-gradient eddy fluxes, locally needed to ensure the strict conservation of energy by nonlinear processes. Such up-gradient eddy fluxes cannot be observed in the passive-scalar dynamics, owing to the absence of an energy invariant that would maintain a correlation between the scalar and the stream function, or in other words, impose a retroaction of the scalar advection on velocity: thus the passive scalar is able to obey the spectral law predicted by simple self-similarity arguments, while vorticity is not. But note that energy conservation by itself does not explain the steep enstrophy spectra, as shown by our 'random phase model' experiment: it is the localness in physical space, associated with energy conservation, that enables coherent structures to form and produce strong spectral steepness. This effect of coherent vortices on the spectral slope cannot be properly reproduced by statistical closure models which also assume a random distribution of phases.

The coherent vortices which appear in the enstrophy inertial range are so strong that the slope of the energy spectrum just reflects their distribution in amplitude and scale. This means that the activity of the flow is mainly concentrated in a hierarchy of vortices which occupy a very small portion of the physical domain, but nevertheless determine the straining timescales. Then the weakly excited vorticity field around and in between vortices can be expected to behave as a passive scalar: this speculation is indeed corroborated by our clipping analysis, which indicates, after removing vortices, a background enstrophy spectrum followings the k^{-1} law. In other words, in spite of the differences noted above and producing the vortices, vorticity dynamics remains a passive-scalar dynamics almost everywhere. This separation of the vorticity field into an active component determining the nonlinear timescales, and a passive component submitted to the cascade process, makes the concept of an universal power law not obviously relevant to the enstrophy inertial range (on this point, see also Babiano *et al.* 1985). The almost exclusive attention focused on the power spectrum during two decades was probably a consequence of the popularity of statistical closures during this period and the fact that the slopes of the power spectrum is the only flow characteristic that can be analysed by the closure approach. Clearly, the power spectrum is an incomplete signature of the dynamical behaviour; the distribution of coherent vortices, their generation processes and stability properties play an essential role.

We do not know yet how the energy distribution of the coherent vortices in the enstrophy inertial range is determined. The relatively large fluctuations of the spectral slope from one experiment to another, depending on the location and nature of the forcing, tend to support the non universality of the distribution law, at least near the injection scale. A more convincing study of this problem would require higher-resolution experiments to look for asymptotic laws. The other problem is the investigation of the energy inertial range, in which the fate of coherent structures has not yet been adequately studied by numerical modelling.

The authors would like to thank G. Holloway, whose comments led to several improvements of the text. The computations were performed at the LMD with the help of R. M. Philippe. The manuscript was typed by M. C. Lanceau and M. C. Cally.

REFERENCES

BABIANO, A., BASDEVANT, C. & SADOURNY, R. 1985 Structure functions and dispersion laws in two-dimensional turbulence. *J. Atmos. Sci.* **42**, 941–949.

BASDEVANT, C., COUDER, Y. & SADOURNY, R. 1985 Vortices and vortex couples in two-dimensional turbulence. In *Macroscopic Modelling of Turbulent Flows*. Lecture Notes in Physics, vol. 230, pp. 327–346. Springer.

BASDEVANT, C., LEGRAS, B., SADOURNY, R. & BELAND, M. 1981 A study of barotropic model flows: intermittency waves and predictability. *J. Atmos. Sci.* **38**, 2305–2326.

BASDEVANT, C., LESIEUR, M. & SADOURNY, R. 1978 Subgrid-scale modeling of enstrophy transfer in two-dimensional turbulence. *J. Atmos. Sci.* **35**, 1028–1042.

BATCHELOR, G. K. 1969 Computation of the energy spectrum in homogeneous two-dimensional turbulence. *Phys. Fluids Suppl.* **12**, II 233.

BRACHET, M. E., MENEGUZZI, M. & SULEM, P. L. 1986 Small-scale dynamics of the high Reynolds number two-dimensional turbulence. *Phys. Rev. Lett.* **57**, 683–686.

CORCOS, G. M. 1983 The prevalence of two-dimensional motion in the turbulent mixing layer. *J. Méc. Theor. Appl.*, Numéro spécial 1983.

COUDER, Y. 1984 Two-dimensional grid turbulence in a thin liquid film. *J. Phys. Lett.* **45**, 353–360.

DESBOIS, M. 1975 Large-scale kinetic energy spectra from Eulerian analysis of Eole wind data. *J. Atmos. Sci.* **32**, 1838–1847.

FORNBERG, B. 1977 A numerical study of 2-D turbulence. *J. Comput. Phys.* **25**, 1–31.

FRISCH, U. 1987 Fully developed turbulence: where do we stand? *Proc. Peyresq 1984 Meeting on Dynamical systems* (ed. S. Diner). Springer (in press).

FRISCH, U. & SULEM, P. L. 1984 Numerical simulation of the inverse cascade in two-dimensional turbulence. *Phys. Fluids* **27**, 1921–1923.

HERRING, J. R. & MCWILLIAMS, J. C. 1985 Comparison of direct numerical simulation of two-dimensional turbulence with two-point closure: the effects of intermittency. *J. Fluid Mech.* **153**, 229–242.

HOLLOWAY, G. & HENDERSHOTT, M. C. 1977 Stochastic closure for nonlinear Rossby waves. *J. Fluid Mech.* **82**, 747–765.

HOLLOWAY, G. & KRISTMANNSSON, S. S. 1984 Stirring and transport of tracer fields by geostrophic turbulence. *J. Fluid Mech.* **141**, 27–50.

KIDA, S. 1985 Numerical simulation of two-dimensional turbulence with high-symmetry. *J. Phys. Soc. Japan* **54**, 2840–2854.

KRAICHNAN, R. H. 1967 Inertial ranges in two-dimensional turbulence. *Phys. Fluids* **10**, 1417–1423.

KRAICHNAN, R. H. 1971 Inertial ranges in two- and three-dimensional turbulence. *J. Fluid Mech.* **47**, 525–535.

LEGRAS, B. 1980 Turbulent phase shift of Rossby waves. *Geophys. Astrophys. Fluid Dyn.* **15**, 253–281.

LEITH, C. E. 1968 Diffusion approximation for two-dimensional turbulence. *Phys. Fluids* **11**, 671–673.

LEITH, C. E. 1985 Two-dimensional coherent structures. *Turbolenza e Predicibilita nella Fluidodinamica Geofisica e la Dinamica del Clima*. Scuola Internazionale di Fisica Enrico Fermi, LXXXVIII, pp. 266–280. Societa Italiana di Fisica. North-Holland.

LESIEUR, M. & HERRING, J. 1985 Diffusion of a passive scalar in two-dimensional turbulence. *J. Fluid Mech.* **161**, 77–95.

LIN, C. C. 1967 *The Theory of Hydrodynamic Stability*. Cambridge University Press.

MCINTYRE, M. E. & SHEPHERD, T. G. 1987 An exact local conservation theorem for finite-amplitude disturbances to non-parallel shear flows, with remarks on Hamistonian structure and on Arnold's stability theorem. *J. Fluid Mech.* **181**, 527–565.

MCWILLIAMS, J. C. 1984 The emergence of isolated coherent vortices in turbulent flow. *J. Fluid Mech.* **146**, 21–43.

MONIN, A. S. & YAGLOM, A. M. 1965 *Statistical Fluid Mechanics* (ed. J. L. Lumley), vol. 2. MIT Press. (Revised and augmented edition from Russian original *Statisticheskaya Gidromekhamika*. Moscow: Nauca, 1965.)

MOREL, P. & LARCHEVÊQUE, M. 1974 Relative dispersion for constant-level balloons in the 200 mb general circulation. *J. Atmos. Sci.* **31**, 2189–2196.

POUQUET, A., LESIEUR, M., ANDRÉ, J. C. & BASDEVANT, C. 1975 Evolution of high Reynolds number two-dimensional turbulence. *J. Fluid Mech.* **72**, 305–319.

RHINES, P. B. 1975 Waves and turbulence on a beta-plane. *J. Fluid Mech.* **69**, 417–443.

RHINES, P. & YOUNG, W. 1982 Homogenization of potential vorticity in planetary gyres. *J. Fluid Mech.* **122**, 347–367.

RHINES, P. & YOUNG, W. 1983 How rapidly is a passive scalar mixed within closed streamlines? *J. Fluid Mech.* **133**, 133–145.

SADOURNY, R. 1985 Quasi-geostrophic turbulence, an introduction. *Turbolenza e Predicibilità nella Fluidodinamica Geofisica e la Dinamica del Clima.* Scuola Internazionale di Fisica Enrico Fermi, LXXXVIII, pp. 133–158. Società Italiana di Fisica.

SADOURNY, R. & BASDEVANT, C. 1981 Une classe d'opérateurs adaptés à la modélisation de la diffusion turbulente en dimension deux. *C. R. Acad. Sci. Paris* **292 II**, 1061–1064.

SADOURNY, R. & BASDEVANT, C. 1985 Parameterization of subgrid scale barotropic and baroclinic eddies in quasi-geostrophic models: Anticipated Potential Vorticity Method. *J. Atmos. Sci.* **42**, 1353–1363.

SANTANGELO, P., PATERNALO, S. & BENZI, R. 1987 Statistical properties of two-dimensional turbulence. *Europhys. Lett* (in press).

SHEPHERD, T. G. 1987 Non-ergodicity of invisid two-dimensional flow on a beta-plane and on the surface of a rotating sphere. *J. Fluid Mech.* **184**, 289–302.

SOMMERIA, J. 1985 Sur la turbulence bi-dimensionnelle: une approche par la magnétohydrodynamique. Thèse, Université Scientifique et Médicale de Grenoble.

STAQUET, C. & LESIEUR, M. 1987 The mixing-layer and its coherence from the point of view of two-dimensional turbulence. *J. Fluid Mech.* (submitted).

WIIN-NIELSEN, A. 1967 On the annual variation and spectral distribution of atmospheric energy. *Tellus* **19**, 540–559.

WINANT, C. D. & BROWAND, F. K. 1974 Vortex pairing: A mechanism of turbulent mixing-layer growth at moderate Reynolds number. *J. Fluid Mech.* **63**, 237–255.